Molecular engineering of supported vanadium oxide catalysts through support modification

Xingtao Gao and Israel E. Wachs

Zettlemoyer Center for Surface Studies, Department of Chemical Engineering, Lehigh University, 7 Asa Drive, Bethlehem, PA 18015, USA
E-mail: xig2@lehigh.edu; iew0@lehigh.edu

Highly dispersed, multilayered surface metal oxide catalysts ($V_2O_5/MO_x/SiO_2$, M = Ti(IV), Zr(IV) or Al(III)) were successfully synthesized by taking into account various factors that govern the maximum dispersion of metal oxide species on silica. The characterization results revealed that the molecular structures of the surface vanadium oxide species on the modified supports are a strong function of environmental conditions. The surface vanadium oxide species under dehydrated conditions are predominantly isolated VO_4 units, similar to the dehydrated V_2O_5/SiO_2 catalysts. Upon hydration, the surface vanadium oxide species on the modified supports consist of polymerized VO_5/VO_6 units and/or less polymerized $(VO_3)_n$ species, which depend on the vanadia content and the specific second metal oxide loading. The surface V cations are found to preferentially interact with the surface metal (Ti, Zr or Al) oxide species on silica. The V(V) cations in the dehydrated state appear to possess both oxygenated ligands of Si(IV)–O^- and M–O^-. Consequently, the reducibility and catalytic properties of the surface vanadium oxide species are significantly altered. The turnover frequencies of the surface VO_4 species on these modified supports for methanol oxidation to redox products (predominantly formaldehyde) increase by more than an order of magnitude relative to the unmodified V_2O_5/SiO_2 catalysts. These reactivity enhancements are associated with the substitution of Si(IV)–O^- oxygenated ligands by less electronegative M–O^- ligands in the O=V(–O–support)$_3$ structure, which strongly suggests that the bridging V–O–support bonds play a key role in determining the reactivity of the surface vanadium oxide species on oxide supports.

KEY WORDS: supported metal oxide catalyst; surface structure; support effect; *in situ* characterization (Raman spectroscopy, UV-vis-NIR DRS); temperature-programmed reduction (TPR); methanol oxidation

1. Introduction

Supported metal oxides are widely applied in many industrial processes as oxidation and solid acid catalysts. Supported metal oxides consist of a two-dimensional metal oxide overlayer on an oxide support. Among them, supported vanadium oxides constitute a very important group of catalysts that are industrially used for sulfuric acid manufacture, oxidation of *o*-xylene to phthalic anhydride, ammoxidation of alkyl aromatics to aromatic nitriles, and the selective catalytic reduction (SCR) of NO_x emissions with NH_3 to N_2 [1]. Supported vanadia catalysts have also been examined for many other reactions, including methanol oxidation, carbon monoxide oxidation and partial oxidation of hydrocarbons [2,3]. Surface vanadium oxide species exhibit very different reactivity properties depending on the specific oxide support used. For example, the reactivity trends of surface vanadium oxide species as a function of oxide support were determined for [2]:

methanol oxidation: $V_2O_5/ZrO_2,\ V_2O_5/TiO_2 \gg V_2O_5/Al_2O_3 \gg V_2O_5/SiO_2$;

CO oxidation: $V_2O_5/ZrO_2 > V_2O_5/TiO_2 > V_2O_5/Al_2O_3$;

the SCR of NO_x: $V_2O_5/ZrO_2 > V_2O_5/TiO_2 > V_2O_5/Al_2O_3 > V_2O_5/SiO_2$.

These trends imply that it is possible to alter the catalytic properties of vanadium oxide catalysts by changing and modifying the oxide support. The basis for these trends lies in the change at the molecular level of the bridging V–O–S bonds between the active surface vanadium oxide species and the support cations, where the support cations possess different electronegativities [1]. Consequently, molecular engineering of the active surface vanadium oxide species can be realized by modifying the bridging V–O–S bonds.

Silica is widely used as an oxide support for other metal oxides, as well as the major component of many solid acid catalysts. Silica is employed in a great number of acid and oxidation reactions. Amorphous Al_2O_3–SiO_2 is one of the most widely used solid acid catalysts in the oil and chemical industries (*e.g.*, isomerization of olefins, paraffins and alkyl aromatics; alkylation of aromatics with alcohols and olefins; olefin oligomerization and catalytic cracking) [4]. Some other silica-containing catalysts have also been developed for various reactions, which are listed in table 1. Silica as a support is cheap, but quite chemically inert. It possesses some favorable properties such as high surface area and excellent thermal/mechanical stability. Thus, modified silica supports as advanced support materials have been widely applied for a number of reactions, as shown in table 1. For example, TiO_2-modified SiO_2 has been considered as a replacement for pure TiO_2 since such a material possesses enhanced thermal/mechanical stability and high surface area, and is also economically favorable. Therefore, studies of silica supported metal oxides are of great fundamental and practical importance.

1022-5528/02/0200-0243/0

Table 1
Various reactions for silica-based catalysts.

Catalyst[a]	Reaction	Reference
TiO_2/SiO_2	Photoxidation of propane	[5]
TiO_2/SiO_2	Catalytic decomposition of chloroform	[6]
TiO_2/SiO_2	Catalytic decomposition of 1,2-dichloroethane	[7]
TiO_2/SiO_2	Propanol dehydration	[8]
TiO_2/SiO_2	Epoxidation of olefins by TBHP/EBHP	[9–11]
TiO_2/SiO_2	The Clause reaction	[12]
TiO_2/SiO_2	Methanol oxidation	[8,13]
TiO_2–SiO_2	Photodecomposition of chlorinated phenols	[14,15]
TiO_2–SiO_2	Photoreduction of CO_2	[16,17]
TiO_2–SiO_2	Photodecomposition of rhodamine-6G	[18]
TiO_2–SiO_2	Complete photocatalytic oxidation of C_2H_4	[19]
TiO_2–SiO_2	Catalytic decomposition of freon 12	[20]
TiO_2–SiO_2	Isomerization of 1-butene	[21–27]
TiO_2–SiO_2	Isomerization of methyloxiane to propanal	[27]
TiO_2–SiO_2	Methanol dehydration	[28]
TiO_2–SiO_2	Ethene hydration and phenol amination	[24]
TiO_2–SiO_2	Cumene dealkylation and propanol dehydration	[21,29]
TiO_2–SiO_2	Decane hydrocracking	[30]
TiO_2–SiO_2	Solvolysis of *cis*-2,3-epoxybutane	[31]
TiO_2–SiO_2	Ammoximation of cyclohexanone	[32]
TiO_2–SiO_2	Epoxidation of α-isophorone by TBHP	[33,34]
TiO_2–SiO_2	Epoxidation of olefins by TBHP/NBHP/H_2O_2	[31,32,35–40]
TiO_2–SiO_2	Selective oxidation of cyclohexane by TBHP	[41]
TiO_2–SiO_2	Hydroxylation of phenol by H_2O_2	[42]
TiO_2–SiO_2	Oxidation of benzene and toluene by H_2O_2	[42]
ZrO_2–SiO_2	Synthesis of isobutane and isobutene from syngas	[43]
ZrO_2–SiO_2	Photocatalytic isomerization of butene	[44]
ZrO_2/SiO_2	Dehydrogenation of cyclohexanol	[45]
Rh/TiO_2–SiO_2	Benzene hydrogenation	[46]
Ni/TiO_2–SiO_2	CO hydrogenation	[47]
$Pd/Al_2O_3/SiO_2$	Combustion of methane	[48]
$Cu/ZrO_2/SiO_2$	Synthesis of methanol from CO/H_2 and CO_2/H_2	[49]
CrO_3/TiO_2-SiO_2	Ethylene polymerization	[50,51]
V_2O_5/TiO_2-SiO_2	SCR of NO_x with NH_3	[52,53]
$V_2O_5/TiO_2/SiO_2$	SCR of NO_x with NH_3	[54]
V_2O_5/TiO_2-SiO_2	Synthesis of *i*-butylaldehyde from ethanol + methanol	[55]
$V_2O_5/TiO_2/SiO_2$	NO reduction with CO	[56]
$V_2O_5/TiO_2/SiO_2$	Selective oxidation of toluene	[57]
$V_2O_5/TiO_2/SiO_2$	Selective oxidation of *o*-xylene	[58a]
$V_2O_5/TiO_2/SiO_2$	Selective oxidation of ethanol to acetaldehyde	[58b]
NiO–Al_2O_3/SiO_2	Butene dimerization	[59]
NiO–Al_2O_3/SiO_2	Ethene and propene oligomerization	[60]

[a] "–"sign used in these catalyst formulas means "mixed with"; while "/" sign means "supported on".

Many heterogeneous catalysts are multicomponent materials with a wide range of chemical compositions and various phases. The different components serve the purpose of (i) generation of new active sites, (ii) modification of the physico-chemical/reactivity/mechanical properties, and (iii) multifunctionality (*e.g.*, hydrocracking catalysts with an acid function and a (de)hydrogenation function). Understanding the interactions between each component at the interface is very important for the rational design of multicomponent catalysts. However, the investigation of interface interactions is experimentally very difficult because multicomponent systems are often very complex, and the detection and identification of interface layers are complicated by the contributions from the simultaneous presence of bulk phases. Thus, it would be interesting to design a catalyst system with two different molecularly thin metal oxide layers on an inert support surface (*i.e.*, silica). The resultant model catalysts, the so called multilayered surface metal oxide catalysts, will allow us to easily investigate the interface interactions between the two surface metal oxide layers on a molecular-level by spectroscopic techniques without interference from coexisting bulk phases. The design of the multilayered surface metal oxide catalysts is also in line with molecular engineering of the active surface vanadium oxide species by modification of the silica support with a specific metal oxide. The present paper will summarize the main results from three different multilayered catalyst systems ($V_2O_5/TiO_2/SiO_2$, $V_2O_5/ZrO_2/SiO_2$ and $V_2O_5/Al_2O_3/SiO_2$) to provide fundamental understanding about the supported metal oxide catalysts.

2. The support effect

The function of the oxide support (*e.g.*, SiO_2, Al_2O_3, TiO_2, *etc.*) in supported metal oxide catalysts is to tailor the catalytic performance of the active metal oxide component (*e.g.*, oxides of V, Mo, Cr, *etc.*) by increasing the number of exposed active sites and/or modifying their molecular structures/physico-chemical properties. The support effect has been associated with the bridging V–O–S bonds, where the eletronegativity of the support cation varies [1].

The electronegativity is usually used to predict the direction and approximate extent of the polarity of a covalent bond [61]. The absolute electronegativity χ is defined as an average of the ionization potential (the energy required to remove an electron from an atom) and the electron affinity (the energy released by gain of one electron) [62], and is further related to the electron chemical potential by [63,64]:

$$\mu = \left(\frac{\partial E}{\partial N}\right)_Z = -\chi,$$

where N is the total number of electrons of an atom or molecule, E is the total electronic energy and Z is the nuclear charge. The physical importance of electronegativity is that the electronegativity differences determine the charge transfer that occurs on bond formation [63].

Relative values of electronegativity have been derived either from experimental data, such as ionization energies and electron affinities, heats of reaction and bond energies, or from theoretical calculations, such as the relative compactness of electronic clouds and the effective nuclear charge at the surface of metals. Despite the different scales used (Pauling, Mulliken and Sanderson), a general order of electronegativity holds for many elements and ions [65].

Sanderson's electronegativity, which is based on the relative compactness of electronic spheres, has been subjected to quantitative testing and has been successfully applied to calculate bond energies of many compounds [66]. The ratio of the average electronic density of an atom to that of an interpolated hypothetical "noble gas" atom of equal number is used as a measure of the relative electronegativity [61]. The change corresponding to the acquisition of unit charge (ΔS) is equal to $1.57S^{1/2}$, where S is Sanderson's relative electronegativity. To obtain the value of the intermediate electronegativity for a compound, the principle of electronegativity equalization can be used, which states that "when two or more atoms initially different in electronegativity combine chemically, they become adjusted to the same, intermediate electronegativity within the compound" [67]. This intermediate electronegativity within the compound is postulated as the geometric mean of the initial electronegativities of all the compound atoms. The equalization principle corresponds to equalization of chemical potentials in a compound since the electronegativity is the negative of the chemical potential [61].

The partial charge δ on an atom in a molecule or a polyatomic ion is a useful parameter in evaluating the effectiveness of the atom as an electron donor or acceptor. It is defined as the ratio of the change in electronegativity in forming the compound to the unit charge change, and the partial charges will add to zero for a neutral molecule [61b,68]. Oxygen in most compounds usually possesses a negative value (electron donor), and with a relatively low negative partial charge of oxygen, the molecule or ion becomes more acidic or less effective as an electron-pair donor [61b]. Therefore, the comparison of oxygen partial charge δ_O in a metal oxide compound as well as its electronegativity can be used to predict the change in the electron density when the ligand of the central cation changes. In contrast, the V(V) cation usually possesses a positive partial charge, which demonstrates its ability as an electron-pair acceptor.

Table 2
Electronegativities and partial charges in some V-containing model clusters.

Molecules/clusters	S	δ_O	δ_V
$VO(OH)_3$	3.06	−0.20	0.22
$VO(OH)_2(OCH_3)$	2.94	−0.24	0.17
$VO(OH)(OCH_3)_2$	2.88	−0.26	0.15
$VO(OCH_3)_3$	2.83	−0.27	0.13
$VO[OSi(OH)_3]_3$	3.01	−0.22	0.20
$VO[OTi(OH)_3]_3$	2.89	−0.26	0.15
$VO[OZr(OH)_3]_3$	2.72	−0.31	0.08

The electronegativities and partial charges of some V-containing model clusters are calculated and presented in table 2. As the OH^- ligand of the $VO(OH)_3$ cluster is substituted by CH_3O^-, the electronegativity and the positive partial charge on vanadium (δ_V) of the cluster decrease, while the negative partial charge on oxygen δ_O becomes more negative. This trend indicates that change of the ligand around the central cation can greatly affect its local chemical environment. Similarly, when using model Ti, Zr, Si hydroxyl clusters as ligands for V(V) cation, the resulting electronegativity is a strong function of the electronegativity of the bridged metal cations (Si > Ti > Zr). This trend reveals that for vanadium oxide compounds, the electron density around both the oxygen and vanadium atoms varies with ligands that possess different electronegativites. Decreasing the electronegativity of the support cations increases the electron density (the negative partial charge δ_O) of the bridging oxygen of the V–O–S bond, which is associated with the significant increase in TOFs for methanol oxidation over the corresponding supported vanadia catalysts. This is the molecular basis for modification of catalytic properties of supported vanadium oxide catalysts.

3. Synthesis of highly dispersed metal oxides on silica

Modification of the silica surface as well as the physico-chemical and reactivity properties of silica supported metal oxides have been active areas of research in the literature. It is somewhat difficult to prepare highly dispersed metal oxide overlayers on silica because of the relatively inert nature of the silica surface. Great effort was devoted to the

synthesis of highly dispersed metal oxide species on silica (TiO_2/SiO_2, V_2O_5/SiO_2, ZrO_2/SiO_2 and Al_2O_3/SiO_2), which were successfully prepared by the incipient wetness impregnation of organic solutions of the corresponding reactive H-sequestering precursor molecules [69,71–73]. Various experimental factors that govern the maximum dispersion capacity of metal oxides on silica were taken into account and have been discussed in detail elsewhere [69]. These are:

(1) maximum surface concentration of the Si–OH hydroxyls;

(2) pretreatment temperature, which should be optimal for removal of physisorbed H_2O molecules and maintaining the maximum Si–OH hydroxyl concentration on silica;

(3) reactivity of the precursor molecules;

(4) reaction time between the precursor molecules and the surface hydroxyls;

(5) maximum monolayer coverage of the precursor molecules.

Through proper control of the above factors, experimental monolayer dispersions of titanium and vanadium oxides on silica were reached at ∼4 Ti atoms/nm^2 and ∼2.6 V atoms/nm^2, respectively [69,71]. However, no attempt was made to determine the maximum dispersion of surface zirconium oxide and surface aluminum oxide species on silica since the techniques employed in this study (Raman and UV-vis DRS spectroscopies) are not sensitive enough to sharply distinguish these surface metal oxide species on silica from their bulk phases. Nevertheless, these metal oxide species on silica are predominantly surface species below surface densities of ∼4 atoms/nm^2 for AlO_x species and 2.5 atoms/nm^2 for ZrO_x species [72,73], as evidenced by the linear relationship of the XPS M/Si surface atomic ratio as a function of the cation surface density shown in figure 1. It is interesting to note that the slopes of the three lines are quite different with the surface zirconium oxide species exhibiting the highest M/Si XPS surface ratio and the surface titanium oxide species the lowest surface ratio at the same cation surface density. This phenomenon might be associated with the different dispersion of the surface metal oxide species with titanium oxide species penetrating deeper into the channels or pores of the silica support that is out of the XPS detection sight. An alternative explanation is that a factor error has been introduced in the experiment and/or calibration, suggesting that the surface compositions derived from XPS analysis may not be comparable between different cations on the support.

The deposition of the surface metal oxide species on silica consumes the surface Si–OH hydroxyls. The consumption of the surface Si–OH hydroxyls, resulting from the surface reaction with the precursor molecules, forms bridging Si–O–M bonds. The relative amounts of remaining isolated Si–OH hydroxyls for various catalysts, represented by the relative intensity of the 7315 cm^{-1} band in the NIR DRS spectra, are shown in figure 2. The results indicate that the surface Si–OH hydroxyls consumed are a strong function of the specific metal oxide species and the metal cation concentration. For the V_2O_5/SiO_2 samples, the isolated surface Si–OH hydroxyls decreases dramatically as the vanadia loading increases, and are almost totally consumed by the deposition

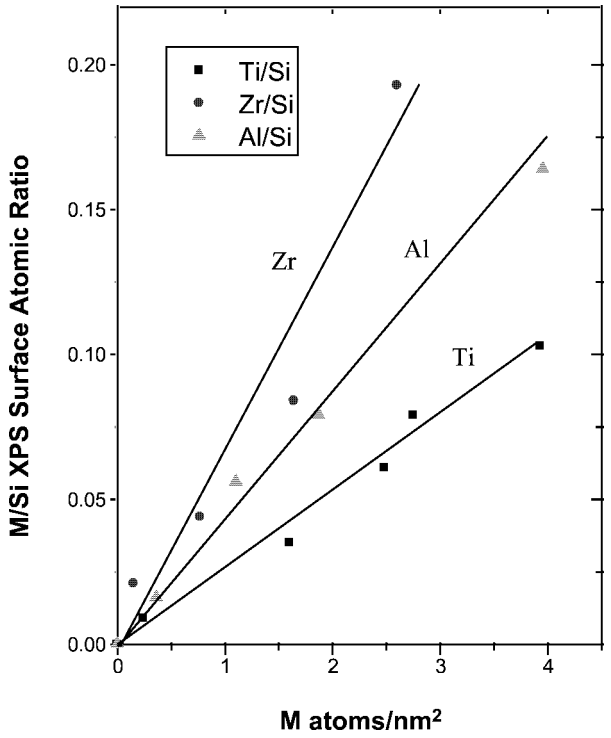

Figure 1. M/Si surface atomic ratio as a function of the cation surface density on silica.

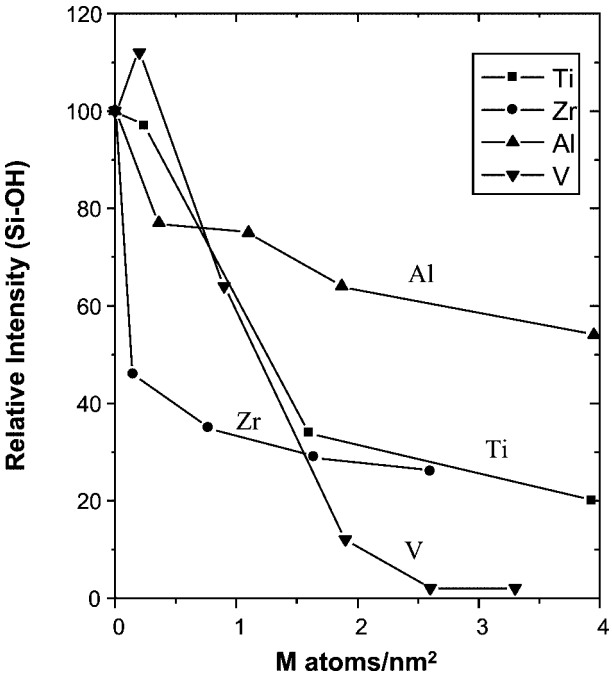

Figure 2. The relative intensity of isolated surface Si–OH hydroxyls (7315 cm^{-1}) as a function of metal cation concentrations.

of V cations at a concentration of 2–2.6 V atoms/nm^2. This result must be associated with the isolated VO_4 structure that possesses three bridging V–O–Si bonds. Changes in the relative intensity of isolated surface Si–OH hydroxyls upon deposition of other metal oxide species (TiO_2, ZrO_2 and Al_2O_3) are significant below 2 metal atoms/nm^2, but are relatively small at higher surface concentrations. The relative amount of isolated surface Si–OH hydroxyls consumed upon deposition of metal oxide decreases in the order: $V_2O_5 > TiO_2 \approx ZrO_2 > Al_2O_3$ at high concentrations ($\geqslant$2 metal atoms/nm^2), which may possibly be associated with the decrease of the average number of Si–O–M bonds per metal cation. The lower consumption of the surface Si–OH hydroxyls by deposition of titanium/zirconium/aluminum oxide species relative to vanadium oxide species suggests that these metal oxide species are probably polymerizing at high loadings, which is consistent with the XANES and UV-vis characterization results for TiO_2/SiO_2 system [69].

4. Structural and reactivity/selectivity properties of surface metal oxides on silica

The molecular structures of the surface metal oxide species on silica were investigated by combined spectroscopic techniques, mainly Raman and UV-vis DRS spectroscopies. Their catalytic properties were examined by methanol oxidation. For the highly dispersed TiO_2/SiO_2 samples, the structure of the surface titanium oxide species is a strong function of environmental conditions as well as titania loading [69]. In the dehydrated state, the surface Ti atoms on the 1% TiO_2/SiO_2 sample are predominantly isolated TiO_4 units; while for the 5% TiO_2/SiO_2 sample, a higher amount of TiO_4 dimer or one dimensional polymerized TiO_4 species may be present; and at monolayer coverage ($\sim$15% TiO_2), two-dimensional polymerized TiO_5 species are dominant. Upon hydration, XANES results show that the average coordination number of the Ti cations increases by about 1, which must be associated with the hydrolysis of some Ti–O–Si bridging bonds. Exposure to the methanol oxidation environment also breaks the Ti–O–Si bridging bonds, resulting in the formation of Ti–OCH_3 and/or Si–OCH_3 species, which are observed by Raman spectroscopy. During methanol oxidation, unlike the catalytic behavior of the bulk titania phase that predominantly possesses acid sites and yields dimethyl ether, the highly dispersed Ti cations on silica act as redox sites since the major reaction products (formaldehyde and methyl formate) are due to the redox sites. The TOF_{redox} of the surface titanium oxide species significantly decreases with increasing TiO_2 loading, demonstrating that the reactivity of the surface Ti sites is a strong function of the molecular structural characteristics. Site isolation and the maximum number of Ti–O–Si bonds per Ti atom for isolated TiO_4 sites are responsible for the highest specific catalytic activity (TOF_{redox}) of 1% TiO_2/SiO_2, whereas polymerization of the surface Ti species decreases the relative fraction of Ti–O–Si bonds and, thus, significantly decreases the activity of the Ti active sites.

The molecular structures of the surface zirconium oxide and aluminum oxide species on silica are less well understood than the surface titanium oxide species. Raman spectra show that the zirconium oxide species on silica possess more Zr–OH hydroxyls in the hydrated state than in the dehydrated state, probably due to the hydrolysis of the Zr–O–Si bonds upon hydration [72]. The catalytic results revealed that the active surface sites on ZrO_2/SiO_2 are predominantly redox sites, whereas the active surface sites on Al_2O_3/SiO_2 are exclusively acid sites [72,73]. The TOF_{redox} of the highly dispersed ZrO_2/SiO_2 catalysts for methanol oxidation to redox products (mainly formaldehyde and methyl formate) is dependent on the zirconia loading, similar to the highly dispersed TiO_2/SiO_2 catalysts. However, the TOF_{dehy} of the highly dispersed Al_2O_3/SiO_2 catalysts for methanol dehydration to dimethyl ether is only slightly dependent on the alumina loading.

The molecular structure of the surface vanadium oxide species on silica is dependent on the environmental conditions, but is independent of the vanadia loading [71]. In the dehydrated state, only the isolated VO_4 species are present up to monolayer coverage of $\sim$12 wt% V_2O_5 ($\sim$2.6 V atoms/nm^2). The three-member rings on silica appear to be the most favorable sites for anchoring the isolated, three-legged $(SiO)_3V{=}O$ units. Hydration dramatically changes the molecular structure of the surface vanadium oxide species, and the degree of hydration plays a critical role in determining the specific structure of the hydrated vanadium oxide species on the silica surface. During the hydration process, hydrolysis of the V–O–Si bonds occurs and V(V) cations may form polymeric chains *via* oligomerization. Full hydration results in maximum polymerization to form chain and/or two-dimensional VO_5/VO_6 polymers, most likely through V–OH–V bridges, which are structurally similar to the $V_2O_5{\cdot}nH_2O$ gels. Under methanol saturation conditions at room temperature, the surface vanadium oxide species may form polymerized chain and/or two-dimensional VO_5/VO_6 units through V–OCH_3–V bridges on the silica surface. Methanol chemisorption at high temperatures ($\geqslant$120 °C) results in isolated, four-fold coordinated V(V)–methoxy species, which may serve as the intermediate complex for methanol oxidation to redox products.

In summary, the deposition of the surface metal oxide species on silica consumes the Si–OH hydroxyls via surface reaction with the precursor molecules to form M–O–Si bonds. The molecular structures of the surface metal oxide species on silica are very different from the corresponding bulk oxide phases and are sensitive to the environmental conditions (*e.g.*, hydration, dehydration and reaction environments). Consequently, the surface metal oxide species on silica possess different reactivity/selectivity properties from their corresponding bulk metal oxide phases. However, these surface metal oxide species on silica do not appear to be very stable at high metal oxide loadings and tend to aggregate during methanol oxidation, which may be associated with the fact that the M–O–Si bridging bonds can be broken upon hydration and methanol chemisorption.

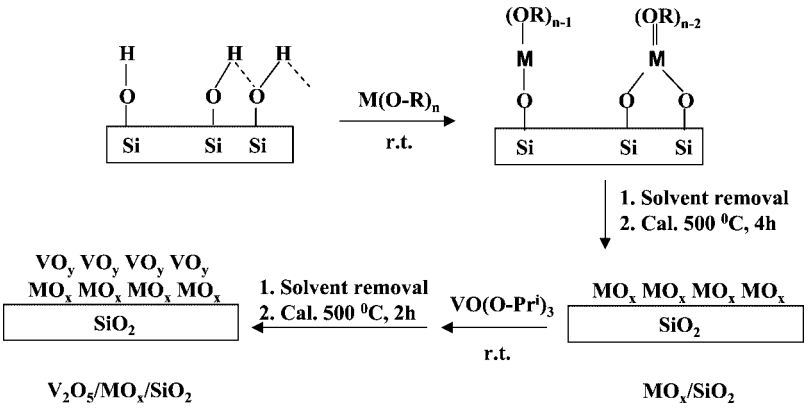

Figure 3. Schematic drawing of the preparation procedure for multilayered $V_2O_5/MO_x/SiO_2$ catalysts.

5. Design and synthesis of multilayered surface metal oxides on silica

Multilayered surface metal oxide catalysts are designed to control their catalytic properties through chemical bonding at the interface between a surface layer of active oxide species (second layer) and a subsurface layer (first layer) of another metal oxide on the SiO_2 support. The highly dispersed multilayered metal oxide phases are not a simple extension of monolayer systems due to possible synergistic interactions. They are also very different from ill-dispersed metal oxide phases on the support surface that contain crystalline particles, which is the case for most of the previous investigations [52–58]. The initial surface metal oxide layer must possess surface hydroxyls that allow the subsequent anchoring of the second metal oxide layer. Therefore, titanium oxide, zirconium oxide and aluminum oxide which possess terminal hydroxyls M–OH instead of terminal M=O bonds are used as the first surface layer. Vanadium oxide is employed as the second surface layer in the present research because of its wide industrial applications as well as its unique and simple well-documented structure on the dehydrated silica surface (*i.e.*, an isolated VO_4 structure). Thus, the silica support is initially modified with a monolayer of surface metal oxide species (TiO_2, ZrO_2 or Al_2O_3), and the surface vanadium oxide species is subsequently dispersed on top of the surface metal oxide species as the second surface layer, as schematically shown in figure 3.

6. Structural and reactivity/selectivity properties of highly dispersed $V_2O_5/MO_x/SiO_2$ catalysts

The molecular structures of the surface vanadium oxide species as well as interfacial interactions between surface vanadium oxide and surface titanium/zirconium/aluminum oxide species were extensively investigated by combined spectroscopic techniques [70,72,73]. TPR and methanol oxidation were employed as chemical probe reactions to examine the reducibility and reactivity/selectivity properties of these multilayered surface metal oxide catalysts.

The characterization results revealed that the molecular structures of the surface vanadium oxide species on these modified supports (MO_x/SiO_2) are a strong function of environmental conditions. In the dehydrated states, the surface vanadium oxide species are predominantly isolated VO_4 units, similar to the dehydrated V_2O_5/SiO_2 catalysts. Upon hydration, the molecular structures of surface vanadium oxide species on these supports appear to be determined by the net surface pH at point-of-zero charge (pzc) since the surface titanium/zirconium/aluminum oxide species are all somewhat more basic than silica. Thus, the hydrated surface vanadium oxide species consist of less polymerized VO_5/VO_6 units relative to the hydrated V_2O_5/SiO_2, which depend on the vanadia and titania/zirconia/alumina loadings. For example, possible surface structures of the multilayered $V_2O_5/TiO_2/SiO_2$ catalysts under hydrated and dehydrated conditions are illustrated in figure 4 (only coordination spheres around the Ti and V cations are shown). In these multilayered catalyst systems, the surface V cations preferentially interact with the surface titanium/zirconium/aluminum oxide species on the silica surface. This preferential interaction is thought to be partially associated with the higher basicity of the surface M–OH hydroxyls than the Si–OH hydroxyls, which results in a higher reactivity of the M–OH hydroxyls with the V-isopropoxide precursor molecules during the catalyst preparation. There-

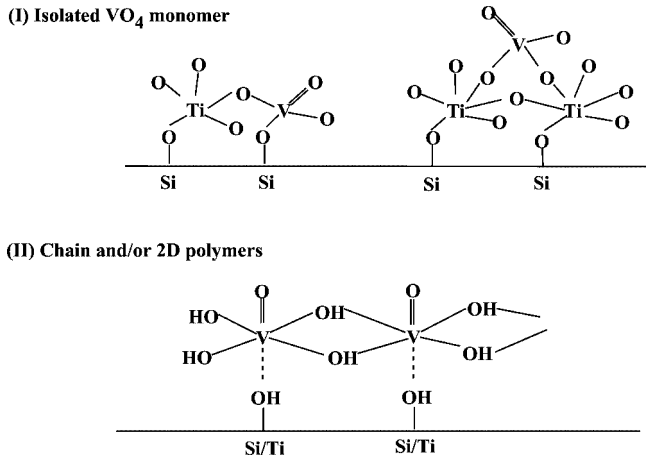

Figure 4. Possible surface structures of the multilayered $V_2O_5/TiO_2/SiO_2$ catalysts in (I) dehydrated and (II) hydrated states.

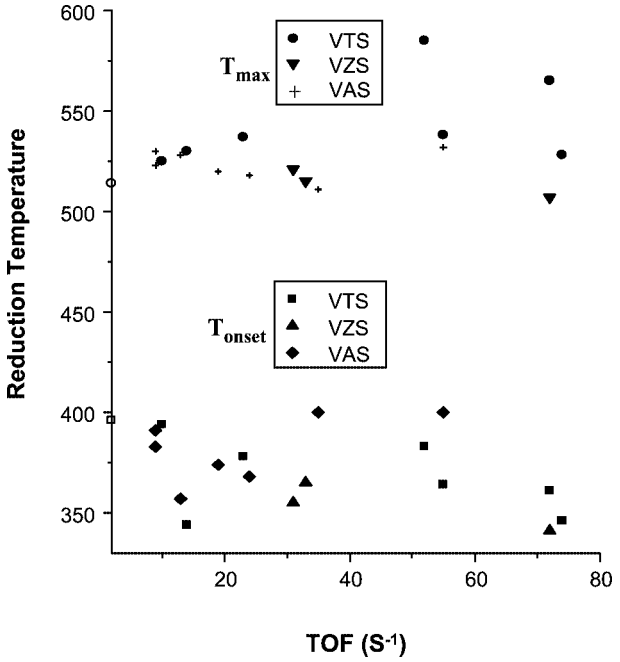

Figure 5. Plots of methanol oxidation TOFs *versus* hydrogen reduction temperatures (T_{onset} and T_{max}) (VTS – $V_2O_5/TiO_2/SiO_2$, VZS – $V_2O_5/ZrO_2/SiO_2$ and VAS – $V_2O_5/Al_2O_3/SiO_2$. The two points on the *Y* axis correspond to 1% V_2O_5/SiO_2).

fore, the V(V) cations in the dehydrated state appear to possess both Si(IV)–O^- and M–O^- oxygenated ligands.

The reducibility and catalytic properties of the surface vanadium oxide species are significantly altered by the modification of the silica surface. The methanol oxidation TOF_{redox} of these multilayered $V_2O_5/MO_x/SiO_2$ catalysts generally increases by more than an order of magnitude relative to the V_2O_5/SiO_2 catalysts. These reactivity enhancements for methanol oxidation are associated with the change of the Si(IV)–O^- oxygenated ligands by the less electronegative M–O^- ligands, which strongly suggests that the basis for the support effect lies in the increase of the electron density of the bridging oxygen of the V–O–support bond. No apparent correlation, however, was found between the TPR reducibility and methanol oxidation reactivity of the $V_2O_5/MO_x/SiO_2$ catalysts whose active V sites possess the same isolated VO_4 structure. As shown in figure 5, both initial and maximum reduction temperatures are irregularly distributed with respect to the TOF values of various supported vanadium oxide catalysts, which strongly suggests that the reducibility obtained by hydrogen reduction is not a suitable parameter for evaluating the reactivity of supported vanadium oxide catalysts for methanol oxidation. This may be related to the fact that the reaction mechanism of hydrogen reduction and experimental conditions of the TPR process are completely different from the methanol oxidation reaction mechanism and the steady-state reaction condition. Differences in hydrogen reduction temperatures are associated with hydrogen dissociative adsorption and diffusion as well as the oxygen availability on the catalysts. Whereas for methanol oxidation, the TOFs of the various supported vanadium oxide catalysts are not only related to the rate determining step that is involving the C–H cleavage of the V–methoxy intermediate species and the oxygen availability, but also depend on the methanol adsorption equilibrium.

The main results of the multilayered surface metal oxide catalysts are summarized below:

- highly dispersed and multilayered surface metal oxide catalysts ($V_2O_5/MO_x/SiO_2$) were successfully synthesized;
- the surface V cations preferentially interact with the surface Ti/Zr/Al oxide species because of their more basic character relative to silica;
- deposition of the V cations on TiO_2/SiO_2 changes the coordination geometry of the surface Ti cations, and the formation of the V–O–Ti bridging bonds is observed by Raman spectroscopy;
- the molecular structures of the surface vanadium oxide species on MO_x/SiO_2 are sensitive to the environmental conditions (hydration, dehydration, methanol chemisorption/oxidation reaction);
- the dehydrated surface vanadium oxide species on MO_x/SiO_2 are predominantly isolated VO_4 groups with both Si(IV)–O^- and M–O^- oxygenated ligands (the same surface structure for all three catalyst systems);
- the methanol oxidation TOF_{redox} of $V_2O_5/MO_x/SiO_2$ increases by more than an order of magnitude relative to V_2O_5/SiO_2, which is related to the substitution of the Si(IV)–O^- ligands by the less electronegative M–O^- ligands (a ligand effect rather than a structural effect);
- no apparent correlation was found between the TPR reducibility and the methanol oxidation TOF of the $V_2O_5/MO_x/SiO_2$ catalysts, which is most likely associated with their different reaction mechanisms.

Acknowledgement

This work was funded by the US National Science Foundation Grant CTS-9417981. The UV-vis-NIR DRS experiments were performed on a Varian Cary 5 UV-vis-NIR spectrometer that was supported by the US Department of Energy – Basic Energy Sciences, Grant DE-FG02-93ER14350. The authors would like to thank Dr. J.L.G. Fierro for XPS analysis and Dr. Miguel A. Banares for chemical analysis and BET measurements.

References

[1] I.E. Wachs, Catalysis 13 (1997) 37.
[2] G. Deo, I.E. Wachs and J. Haber, Crit. Rev. Surf. Chem. 4 (1994) 141.
[3] M. Banares, X.T. Gao, J.L.G. Fierro and I.E. Wachs, Stud. Surf. Sci. Catal. 110 (1997) 295.
[4] A. Corma, Chem. Rev. 95 (1995) 559.
[5] S. Yoshida, S. Takenaka, T. Tanaka, H. Hirano and H. Hayashi, in: *11th Int. Congress on Catalysis*, Stud. Surf. Sci. Catal., Vol. 101 (Elsevier, Amsterdam, 1996) p. 871.

[6] T. Liu and T. Cheng, Catal. Today 26 (1995) 71.
[7] S. Imamura, H. Tarumoto and S. Ishida, Ind. Eng. Chem. Res. 28 (1989) 1449.
[8] S. Srinivasan, A.K. Datye, M. Hampden-Smith, I.E. Wachs, G. Deo, J.M. Jehng, A.M. Turek and C.H.F. Peden, J. Catal. 131 (1991) 260.
[9] R. Hutter, T. Mallat and A. Baiker, J. Catal. 153 (1995) 177.
[10] R.A. Sheldon and J.A. van Doorn, J. Catal. 31 (1973) 427.
[11] R.A. Sheldon, J. Mol. Catal. 7 (1980) 107.
[12] European patents nos. 0 038 741; 0 060 741.
[13] G. Deo, A.M. Turek, I.E. Wachs, D.R.C. Huybrechts and P.A. Jacobs, Zeolites 13 (1993) 365.
[14] G. Dagan, S. Sampath and O. Lev, Chem. Mater. 7 (1995) 446.
[15] R.W. Matthews, J. Catal. 113 (1988) 549.
[16] H. Inoue, T. Matsuyama, B. Liu, T. Sakata, H. Mori and H. Yoneyama, Chem. Lett. (1994) 653.
[17] M. Anpo and K. Chiba, J. Mol. Catal. 74 (1992) 207.
[18] C. Anderson and A.J. Bard, J. Phys. Chem. 99 (1995) 9882.
[19] X. Fu, L.A. Clark, Q. Yang and M.A. Anderson, Environ. Sci. Technol. 30 (1996) 647.
[20] S. Imamura, T. Higashihara and H. Jindai, Chem. Lett. (1993) 1667.
[21] Z. Liu, J. Tabora and R.J. Davis, J. Catal. 149 (1994) 117.
[22] J.B. Miller, S.T. Johnston and E.I. Ko, J. Catal. 150 (1994) 311.
[23] E.I. Ko, J.P. Chen and J.G. Weissman, J. Catal. 105 (1987) 511.
[24] M. Itoh, H. Hattori and K. Tanabe, J. Catal. 35 (1974) 225.
[25] H. Nakabayashi, Bull. Chem. Soc. Jpn. 65 (1992) 914.
[26] C. Contescu, V.T. Popa, J.B. Miller, E.I. Ko and J.A. Schwarz, Chem. Eng. J. 64 (1996) 265.
[27] A. Molnar, M. Bartok, M. Schneider and A. Baiker, Catal. Lett. 43 (1997) 123.
[28] P.K. Doolin, S. Alerasool, D.J. Zalewski and J.F. Hoffman, Catal. Lett. 25 (1994) 209.
[29] J.R. Sohn and J.H. Jang, J. Catal. 132 (1991) 563.
[30] W.F. Maier, J.A. Martens, S. Klein, J. Heilmann, R. Parton, K. Vercruysse and P.A. Jacobs, Angew. Chem. 108 (1996) 222.
[31] C.B. Khouw, C.B. Dartt, J.A. Labinger and M.E. Davis, J. Catal. 149 (1994) 195.
[32] A. Bendandi, G. Fornasari, M. Guidoreni, L. Kubelkova, M. Lucarini and F. Trifirò, Topics Catal. 3 (1996) 337.
[33] R. Hutter, T. Mallat and A. Baiker, J. Catal. 153 (1995) 665.
[34] R. Hutter, T. Mallat and A. Baiker, J. Chem. Soc. Chem. Commun. (1995) 2487.
[35] Z. Liu, G.M. Crumbaugh and R.J. Davis, J. Catal. 159 (1996) 83.
[36] S. Imamura, T. Nakai, H. Kanai and T. Ito, Catal. Lett. 28 (1994) 277.
[37] S. Imamura, T. Nakai, H. Kanai and T. Ito, J. Chem. Soc. Faraday Trans. 91 (1995) 1261.
[38] S. Imamura, T. Nakai, H. Kanai, T. Shiono and K. Utani, Catal. Lett. 39 (1996) 79.
[39] S. Klein, S. Thorimbert and W.F. Maier, J. Catal. 163 (1996) 476.
[40] R. Hutter, T. Mallat and A. Baiker, J. Catal. 153 (1995) 177.
[41] S. Klein, J.A. Martens, R. Parton, K. Vercruysse, P. Jacobs and W.F. Maier, Catal. Lett. 38 (1996) 209.
[42] A. Keshavaraja, V. Ramaswamy, H.S. Soni, A.V. Ramaswamy and P. Ratnasamy, J. Catal. 157 (1995) 501.
[43] Z. Feng, W.S. Postula, C. Erkey, C.V. Philip, A. Akgerman and R.G. Anthony, J. Catal. 148 (1994) 84.
[44] S.C. Moon, M. Fujino, H. Yamashita and M. Anpo, J. Phys. Chem. 101 (1997) 369.
[45] H.J.M. Bosman, E.C. Kruissink, J. van der Spoel and F. van der Brink, J. Catal. 148 (1994) 660.
[46] M.A. Cauqui, J.J. Calvino, G. Cifredo, L. Esquivias and J.M. Rodriguez-Izquierdo, J. Non-Cryst. Sol. 147/148 (1992) 758.
[47] E.I. Ko, J.P. Chen and J.G. Weissman, J. Catal. 105 (1987) 511.
[48] A.F. Ahlstrom-Silversand and C.U.I. Odenbrand, Appl. Catal. 153 (1997) 157.
[49] I.A. Fisher, H.C. Woo and A.T. Bell, Catal. Lett. 44 (1997) 11.
[50] M.P. McDaniel, M.B. Welsh and M.J. Dreiling, J. Catal. 82 (1983) 98.
[51] S.J. Conway, J.W. Falconer and C.H. Rochester, J. Chem. Soc. Faraday Trans. I 85 (1989) 71.
[52] J.J. Calvino, M.A. Cauqui, G. Cifredo, L. Esquivias and J.A. Perez, J. Mater. Sci. 28 (1993) 2191.
[53] B.E. Handy, A. Baiker, M. Schraml-Marth and A. Wokaun, J. Catal. 133 (1992) 1.
[54] (a) R. Mariscal, M. Galan-Fereres, J.A. Anderson, L.J. Alemany, J.M. Palacios and J.L.G. Fierro, *Environmental Catalysis*, eds. G. Centi et al. (SCI Pub., Rome (Italy), 1995) p. 223;
(b) M.D. Amiridis and J.P. Solar, Ind. Eng. Chem. Res. 35 (1996) 978;
(c) R.A. Rajadhyaksha, G. Hausinger, H. Zeilinger, A. Ramstetter, H. Schmeiz and H. Knözinger, Appl. Catal. 51 (1989) 67;
(d) P. Wauthoz, T. Machej and P. Grange, Appl. Catal. 69 (1991) 149.
[55] B.M. Reddy, E.P. Reddy and B. Manohar, Appl. Catal. 96 (1993).
[56] M. Galan-Fereres, R. Mariscal, L.J. Alemany and J.L.G. Fierro, J. Chem. Soc. Faraday Trans. 90 (1994) 3711.
[57] A.A. Elguezabal and V.C. Corberan, Catal. Today 32 (1996) 265.
[58] (a) C.R. Dias, M.F. Portela, M. Galan-Fereres, M.A. Banares, M.L. Granados, M.A. Pena and J.L.G. Fierro, Catal. Lett. 43 (1997) 117;
(b) N.E. Quaranta, J. Soria, V.C. Corberan and J.L.G. Fierro, J. Catal. 171 (1997) 1.
[59] D. Kiessling, G. Wendt, K. Hagenau and R. Schoellner, Appl. Catal. 71 (1991) 69.
[60] D. Kiessling and G.F. Froment, Appl. Catal. 71 (1991) 123.
[61] (a) R.T. Sanderson, J. Chem. Educ. 65 (1988) 113;
(b) R.T. Sanderson, J. Chem. Educ. 65 (1988) 227.
[62] R.S. Mulliken, J. Chem. Phys. 2 (1934) 782.
[63] R.G. Parr, R.A. Donnelly, M. Levy and W.E. Palke, J. Chem. Phys. 68 (1978) 3801.
[64] R.G. Parr and R.G. Pearson, J. Am. Chem. Soc. 105 (1983) 7512.
[65] R.T. Sanderson, in: *Encyclopedia of Chemistry*, 3rd Ed., eds. C.A. Hampel and G.G. Hawley (Van Nostrand Reihold, New York, 1973) p. 385.
[66] R.T. Sanderson, Inorg. Chem. 25 (1986) 3518.
[67] R.T. Sanderson, in: *Chemical Bonds and Bond Energy*, 2nd Ed., ed. E.M. Loebl (Academic Press, New York, 1976).
[68] R.T. Sanderson, *Polar Covalence* (Academic Press, New York, 1983).
[69] X. Gao, S.R. Bare, J.L.G. Fierro, M.A. Banares and I.E. Wachs, J. Phys. Chem. B 102 (1998) 5653.
[70] X. Gao, S.R. Bare, J.L.G. Fierro and I.E. Wachs, J. Phys. Chem. B 103 (1999) 618.
[71] X. Gao, S.R. Bare, B.M. Weckhuysen and I.E. Wachs, J. Phys. Chem. B 102 (1998) 10842.
[72] X. Gao, J.L.G. Fierro and I.E. Wachs, Langmuir 15 (1999) 3169.
[73] X. Gao and I.E. Wachs, J. Catal. 192 (2000) 18.